
On the Effects of Data Distortion on Model Analysis and Training

Antonia Marcu
Vision, Learning and Control
University of Southampton
am1g15@soton.ac.uk

Adam Prügel-Bennett
Vision, Learning and Control
University of Southampton
apb@ecs.soton.ac.uk

Abstract

Data modification can introduce artificial information. It is often assumed that the resulting artefacts are detrimental to training, whilst being negligible when analysing models. We investigate these assumptions and conclude that in some cases they are unfounded and lead to incorrect results. Specifically, we show current shape bias identification methods and occlusion robustness measures are biased and propose a fairer alternative for the latter. Subsequently, through a series of experiments we seek to correct and strengthen the community’s perception of how distorting data affects learning. Based on our empirical results we argue that the impact of the artefacts must be understood and exploited rather than eliminated.

1 Motivation

Modifying data has become commonplace both when training and analysing models, yet the wider implications are often disregarded. As examples of data modification, on the analysis side we take occlusion robustness and shape bias identification methods. On the training side, we focus on some instances of Mixed Sample Data Augmentation (MSDA), where two images are combined to obtain a new training sample. Visual illustrations of each can be found in Figure 1. In this paper we delve into some of the side-effects of data modification and point out that this practice has resulted in the creation of biased model interpretation tools and poorly informed theories. More specifically, we study a number of assumptions which we show are erroneous and which lie at the heart of the methods we briefly introduce below. Contesting these assumptions has broader implications on the community’s perception of what aspects of the data are important when learning.

Shape-texture bias: Deep models are known to be sensitive to interventions that are imperceptible to humans [35, 14], as well as to other forms of distribution shifts [1, 7, 9]. It has been argued that this is intimately linked to networks tending to use texture rather than shape information [2, 12]. Recently, input distortions have become a popular way of assessing a model’s texture bias. To this end, images are divided into a grid and the resulting patches are randomly shuffled such that information is preserved locally, while the global shape is altered [32, 26, 24, 42]. *It is implicitly assumed that patch-shuffling does not introduce misleading shape or texture that could affect model evaluation.* That is, if a model’s accuracy drops when evaluated on patch-shuffled images, this degradation in performance is entirely attributed to the model’s bias for shape information. Thus, any side-effects of the data manipulation process are considered negligible.

Occlusion robustness: Commonly, occlusion robustness is concerned with the amount of information that can be hidden from a model without affecting its ability to classify [e.g. 36, 28]. A widely adopted proxy for measuring occlusion robustness is through the raw accuracy obtained after superimposing a rectangular patch on an image [6, 10, 40, 43, 21]. We refer to this approach as CutOcclusion throughout the paper. Just as for shape bias, this method relies on information introduced not to interfere with a model’s learnt representations such that a decrease in performance can be directly

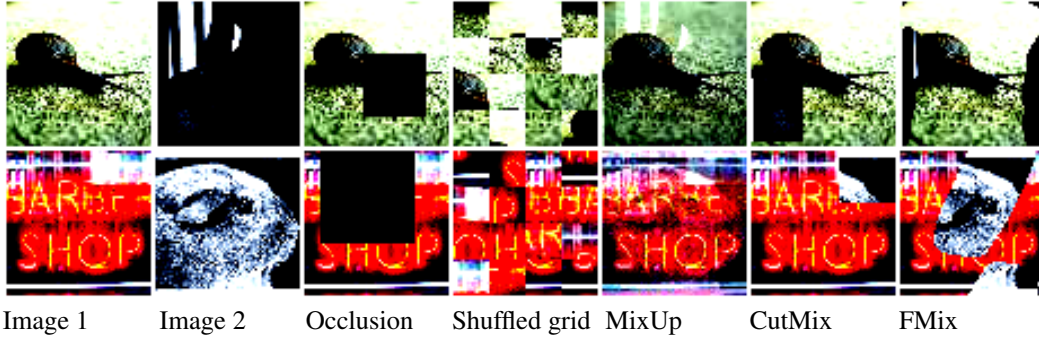


Figure 1: Examples of image distortions. For test-time distortions (Occlusion and Shuffled grid) only Image 1 was used. For mixing augmentations, the first row was generated with a mixing factor of 0.2, while the second one with 0.5.

attributed to lack of robustness. Thus, using CutOcclusion, one implicitly assumes that artefacts do not interfere with the result of robustness evaluation.

Data augmentation studies: In statistical learning, training with augmented data is termed Vicinal Risk Minimisation (VRM) [38, 5] and it is seen as injecting prior knowledge about the neighbourhood of the data samples. The intuition behind augmentation caused researchers to interpret its effect through the similarity between original and augmented data distributions. This perspective is often challenged by methods which, despite generating samples that do not appear to fall under the distribution of natural images, lead to strong learners. Gontijo-Lopes et al. [13] argue it is the *perceived* distribution shift that needs to be minimised, while maximising the sample vicinity. Formalising these concepts, they introduce augmentation “diversity” and “affinity”. Diversity is defined as the training loss when learning with artificial samples, while affinity quantifies the difference between the accuracy on original test data and augmented test data for a reference model. The latter penalises augmentations that introduce artificial information to which the model is not invariant, *implicitly assuming that training with that information is detrimental to generalisation*. Thus, in contrast to the evaluation methods mentioned above, the artefacts are considered non-negligible when training with distorted data.

In summary, it is currently assumed that the artefacts introduced by changes in the data are negligible when evaluating models, while those introduced when training are important and undesirable. These assumptions implicitly shape the community’s perception of how machine learning works. Does the artificial information added by analysis methods not have major side-effects or does it lead to biased results? Conversely, are the artefacts important when training with modified data? Do they cause models to learn better or worse representations?

We set out to answer these questions and find that when the secondary effects of data manipulation are not accounted for, results can be misleading, especially in comparative studies. Taking an oversimplified example to illustrate this for robustness, we can imagine a binary cat–truck image classification problem and two models: model *A*, which identifies cats solely by the presence of ears and model *B*, which has a more holistic approach. Generally, masking out the ears will cause model *A* to misclassify cats and we would consider this model not robust to occlusion, while model *B* will continue to correctly classify them. However, if the ears are covered with a large rectangle that introduces horizontal and vertical edges strongly associated with the truck class, this will cause model *B* to also misclassify. In this case, because the misclassification is not caused by the absence of a feature but rather by the presence of a distractor, we would still consider model *B* robust to occlusion, although its performance degrades. In such a case, CutOcclusion would be unable to distinguish between a model that incorrectly classifies because of lack of information or because of the presence of confounding artefacts, making it an incorrect proxy for measuring occlusion robustness. Thus, the side-effects of data distortion must be taken into account to create fair evaluation methods.

We start by introducing a measure that highlights the existence of such side-effects which we then use to disprove the negligibility of data distortion artefacts when evaluating models. Subsequently, we build on the importance of artefacts to construct empirical counter-examples which disprove common

beliefs in the augmentation literature and highlight the importance of understanding the changes data manipulation introduces. Our contributions are:

- We show that increasingly popular model interpretation and analysis methods are biased, relying on unfounded assumptions (Section 2);
- For measuring occlusion robustness, we propose a fairer alternative (Section 3);
- We show that, in contrast to what is widely assumed, not preserving the data distribution can lead to learning better representations (Section 4).

While the impact of our practical contributions is straight-forward, we believe combating erroneous research directions and improving understanding is more important for the future development of the field. Correctly understanding the increasingly popular mixed-sample augmentation is essential for trusting its usage in sensitive applications where the data can be out of distribution. But most importantly, we believe this could set a new direction in capturing the relationship between data and learned representations, which could ultimately play a role in understanding generalisation.

2 Are artefacts negligible when analysing classifiers?

In this section we show that artefacts are not negligible, and distorting data at evaluation time could have side-effects previously not considered. More specifically, the artefacts can interfere with the representations learnt by the model, which in turn leads to incorrect evaluation. We highlight this interference by showing that the distortion can be consistently associated with a particular class. We do so by looking at the increase in misclassifications per predicted category. That is, from the number of incorrect predictions of a model evaluated on modified data, we subtract the incorrect predictions when testing on original data. If there is a significant increase for a specific class, it indicates that the distortion introduces features the model associates with that class. We refer to this phenomenon as “data interference”. Considering only positive differences, we denote the increase in the percentage of misclassifications for class c of a given model m by i_c^m . Note that the class c is taken to be that predicted by the classifier. To keep the score within a reasonably consistent range across data sets, we scale i_c^m by the number of classes. We define the Data Interference DI index as

$$DI = \frac{i_{c_{max}}}{\sum_c i_c} i_{c_{max}}, \quad (1)$$

where c_{max} is the class with highest mean increase across all runs. The DI index measures the percentage represented by the dominant class c_{max} weighted by its increase. A high index value indicates a sharp increase for a particular class which is consistent across runs. We associate this with an overlap between introduced artefacts and learnt representations, thus highlighting the *side effects of distorting data for model evaluation*. In Appendix B.1 we experiment with an alternative index, where we weight by the highest increase of a model across the 5 runs, so as to obtain a worst-case analysis. As expected, we observe a more accentuated bias in this case.

To obtain models with different behaviours in a controlled manner, we make use of data augmentation. Since it is sufficient to identify some common cases in which models are disfavoured, we choose to reduce our environmental impact by restricting the analysis to simple MSDAs that combine images without incurring additional computation time or external models. As will be argued in Section 3, we expect the unfairness to be present in most settings, thus the exact choice of augmentation is irrelevant. We focus on two popular MSDAs, MixUp [41] and CutMix [40]. MixUp linearly interpolates between two images to obtain a new training example, while CutMix masks out a rectangular region of an image with the corresponding region of another image. Besides the aforementioned methods, we also employ FMix due to its irregularly shaped masks sampled from Fourier space, which will play an important role in our analysis. Note that although the masking methods sample the size of the occluding patch from the same distribution, in CutMix part of the rectangle can be outside the image, which leads to less occluded samples overall. We refer to models by the augmentations they were trained with and use “basic” to label the models trained without MSDA.

Throughout the paper, we do 5 runs of each experiment with PreAct-ResNet18 [16] as the default architecture. We include results for BagNet [2] and VGG [33] in the Appendices. The main data sets we report results on are CIFAR-10/100 [22], Tiny ImageNet [34], FashionMNIST [39], ImageNet [29]. For ImageNet we use pretrained ResNet-101 models made publicly available by Harris et al. [15].

Table 1: DI index for PreAct-ResNet18 on grid-shuffled images for four different types of models. Results with the highest average are given in *italic* and the lowest in **bold**. Information introduced when shuffling tends to interfere less with the representations of FMix and CutMix models.

	basic	MixUp	FMix	CutMix
CIFAR-10	<i>2.90</i> ± 1.10	2.54 ± 1.29	0.60 ± 0.26	0.33 ± 0.17
CIFAR-100	<i>1.05</i> ± 0.59	0.93 ± 0.44	0.23 ± 0.29	0.11 ± 0.10
Fashion	1.12 ± 0.63	<i>2.73</i> ± 1.64	1.12 ± 0.61	0.70 ± 0.22
Tiny	2.58 ± 4.73	<i>0.54</i> ± 0.27	0.38 ± 0.12	0.14 ± 0.12
ImageNet	0.82	<i>1.49</i>	0.58	—

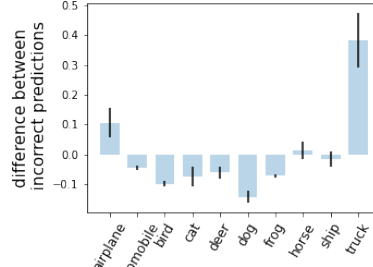


Figure 2: Difference in incorrect predictions on CIFAR-10 for the basic model.

Note that the only experiments for which we are unable to run repeats are those on ImageNet, since only one model per augmentation is provided. For full experimental details, see Appendix A.

2.1 Shape bias

Using the DI metric, we want to show the existence of side-effects that occur when measuring shape bias by the accuracy after patch-shuffling images, which make this evaluation method unreliable. For assessing shape bias through sample manipulation, the standard procedure is to choose between dividing the image in 4, 16 or 64 patches to be shuffled. Since FashionMNIST images are smaller, we choose a 2×2 grid, while for CIFAR-10/100, Tiny ImageNet and ImageNet we use a 4×4 grid. However, similar results are obtained for different grid sizes (Appendix B.2). The large DI index in Table 1 indicates that either basic or MixUp models tend to associate the features artificially introduced by patch-shuffling with a certain class. We take a closer look at the distribution of misclassifications for CIFAR-10 and notice that the basic model tends to wrongly predict the class “Truck” (Figure 2). This is not at all surprising, given that the strong horizontal and vertical edges are highly indicative of this class. Similar observations can be made for other data sets (Appendix B.3). Thus, we believe the grid-shuffling approach is causing models which are not invariant to strong horizontal and vertical edges to appear to rely more heavily on shape information. A model not affected by this transformation could be considered texture-biased if we accept the larger definition of texture as local information. However, there is a question about the extent to which the reciprocal is true; A model can be invariant to the aforementioned edges because it is indeed relying on texture information or simply because it uses different shape-related features.

Is a model necessarily more affected by patch-shuffling if it has a higher shape bias? We will show that the side effects of patch shuffling captured by our DI measure are not necessarily caused by a higher shape bias. To do this, we can use another method of determining shape and texture bias to find a counter-example. We analyse the ImageNet models on the Geirhos Style-Transfer (GST) [12] data set. GST contains artificially generated images where the shape belongs to one class and the texture to another. There are 16 coarse classes that encompass a number of ImageNet categories to which they are mapped. The bias of the models is given by the accuracy obtained when the label is set to either the shape or texture. Using this well-known method of identifying shape bias we want to find models which have similar biases but different DI indices when patch-shuffling. This would indicate that sensitivity to shuffling is not necessarily linked to increased shape bias, which in turn would mean that models evaluated using patch-shuffling can artificially appear more shape biased.

The results in Table 2 show that the basic model does not have a higher shape bias than masking methods although it has a significantly higher DI index, as we have seen in Table 1. We repeat the same experiment on the Tiny ImageNet data set. Geirhos et al. [12] use WordNet [25] to map the 1000 categories to the 16 classes of the GST data set. A number of ImageNet categories that belong to the 16 higher-level classes of GST are missing. For this reason, a poorer overall performance is expected and the results could differ slightly given a better fit between the sets. Nonetheless, we find again no significant correlation between masking augmentation and texture bias. We also include in Table 10 the results for BagNet models, which have smaller receptive fields and so are forced to use more local information. Even in this case, we find a high DI for the basic model and no difference in texture bias

Table 2: Accuracy of augmentation-trained ImageNet and Tiny ImageNet models on the GST data set when the label is taken to be either the shape or texture. There is no clear correlation between masking methods and low texture bias.

	ImageNet		Tiny ImageNet	
	Shape	Texture	Shape	Texture
basic	20.31	53.28	10.56 \pm 0.65	26.04 \pm 1.77
MixUp	24.14	60.31	12.02 \pm 0.33	27.77 \pm 1.56
FMix	21.25	53.43	10.40 \pm 0.39	19.90 \pm 2.12
CutMix	—	—	10.54 \pm 0.38	23.72 \pm 2.42

Table 3: Accuracy obtained on patch-shuffled images. A considerable gap can be noted between the basic model and mask-augmented ones although they exhibit a similar shape bias according to the GST method (Table 2).

	ImageNet	Tiny ImageNet
basic	49.49	13.53 \pm 2.02
MixUp	52.16	17.81 \pm 0.16
FMix	56.20	34.53 \pm 0.62
CutMix	—	42.30 \pm 0.29

compared to MSDA. Thus, a model which is more affected by the side-effects of patch-shuffling is not necessary more shaped-bias. In other words, the artefacts introduced by patch-shuffling can cause models to have different accuracies on these distorted images, albeit not differing in their shape and texture bias.

We verify this conclusion using the GST approach on the two data sets with which this is compatible. Table 3 gives the accuracy obtained when patch-shuffling on Tiny ImageNet and ImageNet. In both cases, for comparable levels of shape and texture bias, different accuracies are obtained. This confirms that *models can appear to have vastly different shape bias when evaluated on randomly rearranged patches, albeit in reality their bias is similar*. Thus, the sensitivity of this approach to artefacts makes it unfair and unreliable.

2.2 Occlusion measurement

We want to determine whether the same issue identified in the case of shape bias evaluation applies to occlusion robustness measures. We focus on CutOcclusion, where a rectangular black patch is superimposed on test images and the robustness is given by the resulting accuracy. We perform the same experiment as before, where the *DI* index is now measured when testing on rectangle-occluded images. There is no standardised distortion when measuring CutOcclusion, with the size and positioning of the obstructing patch varying between studies. Most often in prior art a lack of robustness is noted for large occluders [e.g. 6, 43]. For this reason, we uniformly sample the size of the patch from [0.7, 1], allowing the occluding patch to lie outside the image (as it is done for augmenting with CutMix and CutOut [8]). This allows us to capture both the cases in which either the centre or the border area is masked out but requires a non-uniform distribution to counter for the patches existing outside the image. We also sample from the interval [0.1, 1] where the occluder is restricted to be positioned within the image boundaries and obtain similar results (See Appendix C.1).

Table 4 shows that a significant gap in the *DI* index can be identified for each of the data sets. This indicates that some models will again be disadvantaged. We additionally find that data interference is present for different architectures, when overlapping patches from external images or using differently shaped masks (Appendix B.4). Thus, the result of CutOcclusion and its variants is highly dependent on the problem at hand. That is, whether the artefacts introduced by the artificial occlusion are salient features of the model depends on what features are naturally distinctive for the model. Just as for randomly shuffling tiles, by occluding images using a particularly shaped patch, one implicitly measures a model’s affinity to certain features, albeit those features might be discriminative. This deems such methods inappropriate for fairly assessing robustness and texture bias.

A related observation was made by Hooker et al. [18] who note the pitfalls of manipulating data to determine feature importance. They point out that when simply superimposing uniform patches over image features, it is difficult to assess how much of the reduction in accuracy is caused by the absence of those features and how much is due to images becoming out of distribution. To address this, the most important features identified by an estimator are masked out both on train and test data, closing the gap between the two sets. Hooker et al. then train and evaluate models on the newly generated images. Unlike for interpretability methods, the subject of occlusion robustness studies is the model

Table 4: DI index when occluding with black patches. The highest results are given in italic and the lowest in bold. For each data set, there exists a non-negligible gap in the DI index.

	basic	MixUp	FMix	CutMix
CIFAR-10	<i>1.27</i> ± 0.39	0.49 ± 0.26	0.12 ± 0.07	2.68 ± 2.65
CIFAR-100	<i>1.33</i> ± 0.69	0.36 ± 0.22	0.20 ± 0.31	1.17 ± 0.72
FashionMNIST	0.23 ± 0.12	<i>0.38</i> ± 0.13	0.18 ± 0.14	0.14 ± 0.10
Tiny ImageNet	0.56 ± 0.33	<i>0.40</i> ± 0.07	0.15 ± 0.08	5.04 ± 6.79
ImageNet	0.50	<i>1.50</i>	0.50	–

itself, which makes training with a modified version of the data an inviable option. In the following section we explore ways of overcoming this bias when measuring occlusion robustness.

3 What are fairer alternatives?

We have shown that the results of CutOcclusion depend on whether the artefacts interfere with the learnt representations or not. As we will show in this section, another limitation of CutOcclusion is its sensitivity to the overall generalisation ability of the model. To better reflect how much information can be hidden from a model without affecting its performance, a fair alternative should be invariant to the characteristics of the occluder and to the model’s goodness-of-fit. We propose a simple, more carefully defined measure that aims to decouple the machine’s edge bias and generalisation ability from the occlusion robustness. We refer to our measure as “interplay occlusion” (iOcclusion). Interplay occlusion reflects the change in the interplay between performance on seen and unseen data. Formally,

$$iOcclusion_i = \left| \frac{\mathcal{A}(\mathcal{D}_{train}^i) - \mathcal{A}(\mathcal{D}_{test}^i)}{\mathcal{A}(\mathcal{D}_{train}) - \mathcal{A}(\mathcal{D}_{test})} \right|, \quad (2)$$

where $\mathcal{A}(\mathcal{D})$ denotes the accuracy on a given data set \mathcal{D} , and \mathcal{D}^i is the data set resulting from removing $i\%$ pixels of each image. The intuition is that on train data robust models are less sensitive to the artefacts of the occlusion policy for small levels of occlusion, resulting in a large difference in accuracy from that on unseen data. The performance of both train and test gets close to random as the percentage of occluded data approaches 90% and we expect the gap to fall off quicker for less robust models. This change in interplay is taken with respect to the generalisation gap of the model, such that the quality of the model fit in itself does not interfere with the robustness measure.

Although iOcclusion reduces data interference, other factors have to also be considered when choosing a masking method for computing \mathcal{D}^i , such as the number of contiguous components or the amount of salient information masked out. In this paper we choose to generate masks using Grad-CAM [30], such that the area with most salient $i\%$ pixels is covered. It must be noted that this method implicitly assumes there could be multiple occluders and has the downside of incurring a higher environmental cost. For this, we also experiment with using rectangular or Fourier-sampled masks and conclude that although random masking makes the process noisier, the exact choice of masking method is of secondary importance as long as the occluder’s granularity is accounted for. Appendix C.4 provides discussion and results on these alternative instances of iOcclusion, as well as differences in their carbon footprint. For a fair comparison, throughout this section we do not allow the obstructing patch when measuring CutOcclusion to lie outside the image such that the fraction removed is exact.

Assessing the correctness of such a measure is difficult in the absence of a baseline. For the remainder of this section we will build varied experiments to attest the validity of our method, highlighting two important limitations of CutOcclusion that our approach addresses: sensitivity to the specifics of the occluding patch and sensitivity to model’s generalisation performance. We focus on the key results, but include additional ones and further experiments in Appendix C. Since occlusion in real-life scenarios could be caused by non-uniformly coloured objects, an appropriate measure must generalise across colour patterns. We show that the results of CutOcclusion are sensitive to the colour pattern of the occluding patch, while iOcclusion is more invariant. To see this, we superimpose patches from images belonging to a different data set when computing iOcclusion and CutOcclusion, and compare the results to those obtained when occluding with black patches only. For visual clarity, Figure 3 presents the results for the least and most robust models (see Appendix C.2 for a full comparison).

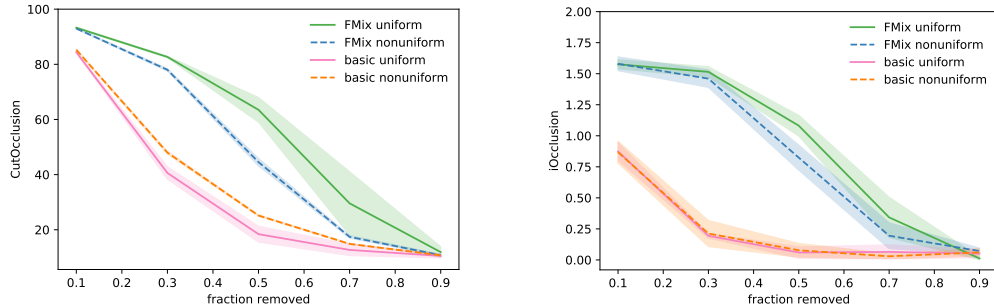


Figure 3: CutOcclusion (left) and iOcclusion (right) when occluding with black patches (uniform) and patches taken from other images (nonuniform). iOcclusion gives more consistent results.

Table 5: DI index and occlusion robustness for models trained on CIFAR-10 when obstructing 30% of the image pixels with non-uniform patches. When measuring the robustness with CutOcclusion, RM appears significantly less robust than CutMix due to its sensitivity to patching with rectangles, while iOcclusion highlights the robustness specific to training with FMix-like masks. Given in bold is the closest result to that of RM for each evaluation.

	basic	MixUp	CutMix	FMix	RM
DI index	1.67 ± 0.27	1.00 ± 0.31	0.17 ± 0.16	0.15 ± 0.03	0.39 ± 0.07
CutOcclusion	47.97 ± 0.52	58.65 ± 1.01	76.56 ± 6.36	78.00 ± 0.45	60.79 ± 5.03
iOcclusion	0.21 ± 0.10	0.57 ± 0.18	1.09 ± 0.17	1.46 ± 0.07	1.20 ± 0.23

For iOcclusion, using uniform occluders gives similar results to its non-uniform version, whereas the CutOcclusion measure provides an inconsistent model evaluation.

As we have argued, in addition to not being sensitive to the colour pattern of the patch, a fair measure must also be invariant to the shape of the patch. To empirically confirm iOcclusion reduces the importance of edge information, we aim to obtain a model that is robust to occlusion, but at the same time has a high DI index (it is sensitive to edge information). To this end, we create a variation of FMix, Random Masks (RM), where at the beginning of the training process three masks are randomly sampled from Fourier space. For each batch, one of the three is chosen uniformly at random. While the RM models are not sensitive to black-patch occlusion, when masking with patterned patches they have a higher DI index than FMix, as desired. Table 5 gives results for a fraction of 0.3 pixels covered by a non-uniform occluder. Our measure reflects the robustness of training with RM, situating it close to other masking methods. On the other hand, because CutOcclusion implicitly penalises models with high DI index, according to this measure RM appears almost as sensitive to occlusion as MixUp. Figure 8 shows results for a wider range of fractions.

Another problem that occurs when purely looking at post-masking accuracy is weaker models would erroneously appear less robust. We show this by reversing the problem: we evaluate the same model on two different subsets of the CIFAR-100 data set: typical and tail images as categorised by Feldman and Zhang [11]. They consider a train-test sample pair to belong to the tail of the data distribution if the test sample is correctly classified when a model is trained with the train sample and incorrectly without it. CutOcclusion would indicate that models are significantly more robust to occluding typical examples. However, a closer analysis makes us doubt this conclusion. The raw accuracy on both train and test data for tail examples is lower than for the typical ones. In fact, the performance when occluding images decreases at the same rate for the two subsets. By way of definition, iOcclusion allows a fair comparison of robustness regardless of the overall performance of a model (Figure 4).

As we evidenced through controlled experiments, there are many cases that CutOcclusion does not properly address. From a model analysis perspective, correctly assessing the occlusion robustness could lead to better understanding and development of models and training procedures. Equally important, it has applicability for real-world deployments where no prior knowledge exists about the possible shapes of the obstructions. While this aspect of generality is the strength of our approach, it must be stressed that when there exists a limited set of known possible occluders, evaluating

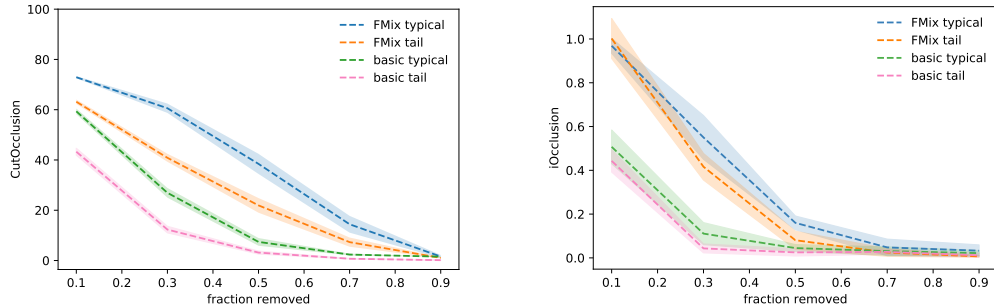


Figure 4: CutOcclusion (left) and iOcclusion (right) for the basic and FMix models on two subsets of the same data set: tail and typical. Evaluating the models with iOcclusion on the two types of samples leads to mostly overlapping robustness levels. That is, they do not differ outside the margin of error. On the contrary, CutOcclusion incorrectly finds the models to be less robust on tail data.

Table 6: Augmentation comparison on CIFAR-10. We consider two variants when calculating diversity. One is computing the cross-entropy loss using the label of the majority class (Diversity), as for mixing in [20]. The alternative, MixDiversity, takes a linear combination of the two cross-entropy losses.

	Affinity	Diversity	MixDiversity
MixUp	-12.58 ± 0.14	0.41 ± 0.01	0.84 ± 0.00
FMix	-25.55 ± 0.26	0.34 ± 0.01	0.65 ± 0.00

Table 7: DI index measured for non-uniform occlusion when training without the class with highest increase in incorrect predictions. Again, a gap can be noted, supporting the idea that data interference is not specific to peculiar cases.

	CIFAR-10	CIFAR-100
MixUp	0.39 ± 0.15	1.22 ± 0.19
FMix	0.08 ± 0.06	0.50 ± 0.21

robustness specifically to them could be safer. Incorrectly assessing robustness can have severe effects especially when applied to sensitive applications such as autonomous vehicles or medical imaging. We do not propose a universal solution, but rather suggest an alternative to the biased approach for the common scenario in which the environment is not controlled and little is known about all the potential occluders. However, even in this case, our metric should be taken as a guide when analysing models. Although iOcclusion aims to address data interference, since a ground-truth does not exist, it cannot be guaranteed that this method provides fair results in the absolute.

The strength of the bias will depend on the data in question and some applications will be more heavily affected than others. We have seen that for natural images this bias does exist. To confirm that we have not just identified isolated cases, we remove the class that has the highest increase in mispredictions and retrain the models on the remaining classes. We find that the bias is again present (Table 7), but with respect to another class. For example, in the case of CIFAR-10, after removing the “Truck” class, models mispredict rectangle-occluded images as “Boat” (Appendix D). Thus, the edge artefacts are very likely to interfere with learnt representations since they are such fundamental features. From an evaluation perspective, as we have seen, this impacts assessment methods and must be accounted for. From the training perspective, such a widespread data interference of masking distortions would indicate a large perceptual shift in the data when performing MSDA. In the following section we investigate the importance of the artefacts in this case and their implications.

4 Is the magnitude of the distribution shift important?

Traditionally it was believed that a good augmentation should have minimal distribution shift. Most recently, it has been argued that it is the degree of the *perceived* shift that determines augmentation quality [13]. We show that *the magnitude of the distribution shift does not determine augmentation quality*. We start with the perceptual gap of training with MSDA, as proposed in Gontijo-Lopes et al. [13]. Reiterating, this is given by the difference between the performance of the baseline model when presented with original test data and augmented test data and is termed “affinity”. Subsequently, we address the gap in the wider sense, as is often sought in prior art. We first argue that high affinity and high diversity are not necessarily desirable. Indeed, on CIFAR-10, we find FMix, a better performing

augmentation, to have both lower affinity and lower diversity than MixUp (Table 6). For diversity, we compute the cross-entropy loss where the label is taken to be that of the majority class. Similar results are obtained with the MixUp loss, where a weighted average of the true labels is taken.

While intuitively for a high level of affinity, high diversity could correspond to better methods, the converse does not hold. We argue this is because affinity is rather an analysis of the learnt representations of the reference model and cannot give an insight into the quality of the augmentation or its effect on learning. The limitations of affinity are intimately linked to those of CutOcclusion. We have seen in Section 3 that the bias of the basic model is present not only when obstructing an image with a uniform patch, but also when mask-mixing. As such, an augmentation will have a lower affinity if it introduces artefacts that could otherwise lead to learning better representations when used in the training process. We believe this issue extends to other approaches that aim to motivate the success of MSDA through reduced distribution shift. Henceforth, we focus on bringing further supporting evidence that the importance lies in the invariance introduced by the shift and its interaction with the given problem rather than its magnitude.

4.1 If it is not the magnitude that matters, is it the direction?

We use empirical evidence to argue against previous assumptions behind the success of MSDA and propose the study of introduced bias as a more informative research direction. Here we use the term “bias” to refer to a drift in the learnt representations introduced by the change in the training procedure. A fundamental difference to classical training is that in the case of augmentation the samples are no longer independent. Mixed-sampling takes this even further. An immediate question is, does the added correlation lead to more meaningful representations? It is claimed that the strength of MixUp lies in causing the model to behave linearly between two images [41] or in pushing the examples towards their mean [4]. Both of these claims rely on the combined images to be generated from the same distribution. We perform inter-dataset augmentation and show that good performance can be obtained even when the source images come from different distributions. The same inter-dataset experiment further shows that by distorting the data distribution by the same magnitude, we can obtain two different results. This suggests that it is the *direction* of the introduced bias that is important for understanding the impact of augmentation.

We use the reformulated objective setting [19, 15], where targets are not mixed and the mixing coefficient is drawn from an imbalanced Beta distribution. This allows us to apply MSDA between data sets. Thus, for training a model on a data set, we use an additional one whose targets will be ignored. As an example, a model that is learning to predict CIFAR-10 images will be trained on a combination of CIFAR-10 and CIFAR-100 images, with the target of the former. This scenario breaks the added correlation between training examples. Note that when mixing between data sets we use the same procedure as when performing regular MSDA, without improving the process.

Table 8 contains the results of this experiment, showing that an accuracy similar to or better than that of regular MSDA can be obtained by performing inter-dataset MSDA. This invalidates the argument that the power of MixUp resides in causing the model to act linearly between samples. Another observation is that for FMix and MixUp, introducing elements from CIFAR-100 when training models on the CIFAR-10 problem does not harm the learning process. The reciprocal, however, does not hold. Hence, the “distribution shift” is more intimately linked to the problem at hand and aiming to characterise an augmentation based on the distance from the original distribution is a limiting approach, especially when the distance is measured as perceived by a reference model.

We believe an explanation is that the artefacts created when putting together images from CIFAR-10 with those of CIFAR-100 could introduce information that makes the separation of the 10 classes easier. However, if the information happens to interfere with a feature that is important for separating the CIFAR-100 categories, the performance could degrade on this data set. This singular experiment is not sufficient to draw any general conclusions. However, it does show that shifting two distributions by the same amount can have different effects on the model performance. Thus, *the specifics of the bias introduced could be more important than its magnitude*. While some level of data similarity has to be preserved when performing MSDA, it is far from being the objective of such data-distorting approaches which, as we will argue further, should be rather seen as forms of regularisation.

We have seen that for all considered data sets, artefacts introduced by masking methods seem to overlap with common features. This has led us to believe that MSDA training could help bypass

Table 8: Accuracy on CIFAR-10 (left) and CIFAR-100 (right) upon mixing with samples from a different data set. The baseline is the accuracy when training with a single data set using the reformulated objective. In the interest of space, CIFAR-110 is used to refer to mixing with CIFAR-100 when training on the CIFAR-10 problem and vice-versa.

	MixUp	FMix	CutMix	MixUp	FMix	CutMix
baseline	94.18 \pm 0.34	94.36 \pm 0.28	94.67 \pm 0.20	74.68 \pm 0.37	75.75 \pm 0.31	74.19 \pm 0.50
CIFAR-110	94.70 \pm 0.27	94.80 \pm 0.32	94.66 \pm 0.12	72.36 \pm 1.04	74.80 \pm 0.55	74.47 \pm 0.39
Fashion	92.28 \pm 0.28	95.03 \pm 0.10	94.61 \pm 0.19	66.40 \pm 1.86	74.46 \pm 0.57	74.06 \pm 0.28

some of the simplicity bias. The simplicity bias refers to the tendency of deep models to find simple representations and has been used to justify the success of deep models [27, 37]. Recent research shows that this propensity causes models to ignore complex features that explain the data well in favour of elementary features, even when they lead to worse performance [31, 17].

Although it could seem natural that since MSDAs are not augmentations in the VRM sense, they will increase the complexity of the problem, we design an experiment to support this claim. Similarly to Shah et al. [31], we combine CIFAR-10 and MNIST [23] samples. Since they have the same number of classes, we can easily associate each class of one data set with a corresponding one from the other. Thus, we stack a padded image from the k th class of MNIST on top of a sample from the k th class of CIFAR-10, such that a $3 \times 64 \times 32$ image is obtained. We then randomly combine the test images and separately compute the accuracy with respect to the targets of each data set.

The predictions with respect to the CIFAR-10 labels are no better than random (10.04 \pm 0.11), while the accuracy with respect to the MNIST images remains high (99.57 \pm 0.72). Thus, models trained on this combination are mostly relying on MNIST images to make predictions. Similar behaviours have previously been associated with simplicity bias. Subsequently, when training, we perform FMix only on MNIST images and observe that this is enough to reverse the results. Evaluating against the CIFAR-10 label gives an accuracy of 86.60 \pm 0.34, while testing against the MNIST label only gives 11.61 \pm 0.30. We find that this also holds true for the other MSDAs. Thus, performing these distortions on the simpler data set increases its complexity to the point where it surpasses that of CIFAR-10.

Previously, we presented evidence that masking MSDA does not necessarily promote learning neither more shape nor texture information. In the light of this fact along with the results from this section, we believe image distortions force the model to learn more complex both shape and texture-specific features. Thus, in this paper we pointed out that the shift in learnt representations can lead to better models and simply quantifying the distribution shift can be misleading. An open question remains: How can we better capture the bias that is introduced and measure its quality? We believe understanding how a relatively small change in the data distribution impacts learnt representations could lead the way to characterising the relationship between data and model generalisation.

5 Conclusions

Distorting data is such a commonplace procedure, yet little effort has been devoted to investigating its broader effects. This is particularly problematic when image modifications are applied in analyses. We show a number of cases in which this leads to *biased results*. For occlusion robustness measurement, we propose an alternative. The insights we gain from this endeavour point towards the study of data characteristics as a cornerstone of our understanding and raise a number of questions about mixed sample data augmentation, on which we subsequently focus. We note that they interfere with features that are consistently found across a number of data sets and conclude that the methods commonly used are forms of mixed sample *regularisation* rather than augmentation. A limitation of previous studies that aim to explain their success is the focus on trying to argue similarity with original data, rather than explaining the bias introduced by the distortion. Correctly interpreting it is important not only for making the models trustable but also for injecting more informed prior knowledge in future applications. Beyond their practical benefits, we believe MSDAs have the potential to help characterise the interplay between data and learnt representations. Overall, the purpose of our paper is to encourage better practice when dealing with all forms of data distortions.

References

- [1] Rocío Alaiz-Rodríguez and Nathalie Japkowicz. Assessing the impact of changing environments on classifier performance. In *Conference of the Canadian Society for Computational Studies of Intelligence*, pages 13–24. Springer, 2008.
- [2] Wieland Brendel and Matthias Bethge. Approximating CNNs with bag-of-local-features models works surprisingly well on imagenet. In *International Conference on Learning Representations*, 2019. URL <https://openreview.net/forum?id=SkfMWhAqYQ>.
- [3] Fabio Maria Carlucci, Antonio D’Innocente, Silvia Bucci, Barbara Caputo, and Tatiana Tommasi. Domain generalization by solving jigsaw puzzles. In *CVPR*, 2019.
- [4] Luigi Carratino, Moustapha Cissé, Rodolphe Jenatton, and Jean-Philippe Vert. On mixup regularization. *arXiv preprint arXiv:2006.06049*, 2020.
- [5] Olivier Chapelle, Jason Weston, Léon Bottou, and Vladimir Vapnik. Vicinal risk minimization. In *Advances in neural information processing systems*, pages 416–422, 2001.
- [6] Sanghyuk Chun, Seong Joon Oh, Sangdoon Yun, Dongyoon Han, Junsuk Choe, and Youngjoon Yoo. An empirical evaluation on robustness and uncertainty of regularization methods. *arXiv preprint arXiv:2003.03879*, 2020.
- [7] David A Cieslak and Nitesh V Chawla. A framework for monitoring classifiers’ performance: when and why failure occurs? *Knowledge and Information Systems*, 18(1):83–108, 2009.
- [8] Terrance DeVries and Graham W Taylor. Improved regularization of convolutional neural networks with cutout. *arXiv preprint arXiv:1708.04552*, 2017.
- [9] Logan Engstrom, Brandon Tran, Dimitris Tsipras, Ludwig Schmidt, and Aleksander Madry. Exploring the landscape of spatial robustness. In *International Conference on Machine Learning*, pages 1802–1811. PMLR, 2019.
- [10] Alhussein Fawzi and Pascal Frossard. Measuring the effect of nuisance variables on classifiers. In Edwin R. Hancock Richard C. Wilson and William A. P. Smith, editors, *Proceedings of the British Machine Vision Conference (BMVC)*, pages 137.1–137.12. BMVA Press, September 2016. ISBN 1-901725-59-6. doi: 10.5244/C.30.137. URL <https://dx.doi.org/10.5244/C.30.137>.
- [11] Vitaly Feldman and Chiyuan Zhang. What neural networks memorize and why: Discovering the long tail via influence estimation. *Advances in Neural Information Processing Systems*, 33, 2020.
- [12] Robert Geirhos, Patricia Rubisch, Claudio Michaelis, Matthias Bethge, Felix A. Wichmann, and Wieland Brendel. Imagenet-trained CNNs are biased towards texture; increasing shape bias improves accuracy and robustness. In *International Conference on Learning Representations*, 2019. URL <https://openreview.net/forum?id=Bygh9j09KX>.
- [13] Raphael Gontijo-Lopes, Sylvia J Smullin, Ekin D Cubuk, and Ethan Dyer. Affinity and diversity: Quantifying mechanisms of data augmentation. *arXiv preprint arXiv:2002.08973*, 2020.
- [14] Ian J Goodfellow, Jonathon Shlens, and Christian Szegedy. Explaining and harnessing adversarial examples. *arXiv preprint arXiv:1412.6572*, 2014.
- [15] Ethan Harris, Antonia Marcu, Matthew Painter, Mahesan Niranjan, Adam Prügel-Bennett, and Jonathon Hare. Understanding and enhancing mixed sample data augmentation. *arXiv preprint arXiv:2002.12047*, 2020.
- [16] Kaiming He, Xiangyu Zhang, Shaoqing Ren, and Jian Sun. Identity mappings in deep residual networks. In *European conference on computer vision*, pages 630–645. Springer, 2016.
- [17] Katherine Hermann and Andrew Lampinen. What shapes feature representations? exploring datasets, architectures, and training. In H. Larochelle, M. Ranzato, R. Hadsell, M. F. Balcan, and H. Lin, editors, *Advances in Neural Information Processing Systems*, volume 33, pages 9995–10006. Curran Associates, Inc., 2020. URL <https://proceedings.neurips.cc/paper/2020/file/71e9c6620d381d60196ebe694840aaaa-Paper.pdf>.

- [18] Sara Hooker, Dumitru Erhan, Pieter-Jan Kindermans, and Been Kim. A benchmark for interpretability methods in deep neural networks. In *Advances in Neural Information Processing Systems*, pages 9737–9748, 2019.
- [19] Ferenc Huszár. mixup: Data-dependent data augmentation, 2017. URL <http://www.inference.vc/mixup-data-dependent-data-augmentation/>.
- [20] Hiroshi Inoue. Data augmentation by pairing samples for images classification. *arXiv preprint arXiv:1801.02929*, 2018.
- [21] Narine Kokhlikyan, Vivek Miglani, Miguel Martin, Edward Wang, Bilal Alsallakh, Jonathan Reynolds, Alexander Melnikov, Natalia Kliushkina, Carlos Araya, Siqi Yan, et al. Captum: A unified and generic model interpretability library for pytorch. *arXiv preprint arXiv:2009.07896*, 2020.
- [22] Alex Krizhevsky et al. Learning multiple layers of features from tiny images. 2009.
- [23] Yann LeCun and Corinna Cortes. MNIST handwritten digit database. 2010. URL <http://yann.lecun.com/exdb/mnist/>.
- [24] Tiange Luo, Tianle Cai, Mengxiao Zhang, Siyu Chen, Di He, and Liwei Wang. Defective convolutional layers learn robust CNNs. *arXiv preprint arXiv:1911.08432*, 2019.
- [25] George A Miller. Wordnet: a lexical database for english. *Communications of the ACM*, 38(11): 39–41, 1995.
- [26] Chaithanya Kumar Mummadi, Ranjitha Subramaniam, Robin Huttmacher, Julien Vitay, Volker Fischer, and Jan Hendrik Metzen. Does enhanced shape bias improve neural network robustness to common corruptions? In *International Conference on Learning Representations*, 2021. URL <https://openreview.net/forum?id=yUxUNaj2S1>.
- [27] Preetum Nakkiran, Gal Kaplun, Dimitris Kalimeris, Tristan Yang, Benjamin L Edelman, Fred Zhang, and Boaz Barak. SGD on neural networks learns functions of increasing complexity. *arXiv preprint arXiv:1905.11604*, 2019.
- [28] Karim Rajaei, Yalda Mohsenzadeh, Reza Ebrahimpour, and Seyed-Mahdi Khaligh-Razavi. Beyond core object recognition: Recurrent processes account for object recognition under occlusion. *PLoS computational biology*, 15(5):e1007001, 2019.
- [29] Olga Russakovsky, Jia Deng, Hao Su, Jonathan Krause, Sanjeev Satheesh, Sean Ma, Zhiheng Huang, Andrej Karpathy, Aditya Khosla, Michael Bernstein, Alexander C. Berg, and Li Fei-Fei. ImageNet Large Scale Visual Recognition Challenge. *International Journal of Computer Vision (IJCV)*, 115(3):211–252, 2015. doi: 10.1007/s11263-015-0816-y.
- [30] Ramprasaath R Selvaraju, Michael Cogswell, Abhishek Das, Ramakrishna Vedantam, Devi Parikh, and Dhruv Batra. Grad-cam: Visual explanations from deep networks via gradient-based localization. In *Proceedings of the IEEE international conference on computer vision*, pages 618–626, 2017.
- [31] Harshay Shah, Kaustav Tamuly, Aditi Raghunathan, Prateek Jain, and Praneeth Netrapalli. The pitfalls of simplicity bias in neural networks. In H. Larochelle, M. Ranzato, R. Hadsell, M. F. Balcan, and H. Lin, editors, *Advances in Neural Information Processing Systems*, volume 33, pages 9573–9585. Curran Associates, Inc., 2020. URL <https://proceedings.neurips.cc/paper/2020/file/6cfe0e6127fa25df2a0ef2ae1067d915-Paper.pdf>.
- [32] Baifeng Shi, Dinghuai Zhang, Qi Dai, Zhanxing Zhu, Yadong Mu, and Jingdong Wang. Informative dropout for robust representation learning: A shape-bias perspective. In *International Conference on Machine Learning*, pages 8828–8839. PMLR, 2020.
- [33] Karen Simonyan and Andrew Zisserman. Very deep convolutional networks for large-scale image recognition. In *International Conference on Learning Representations*, 2015.
- [34] Stanford. Tiny imagenet visual recognition challenge, 2015. URL <https://tiny-imagenet.herokuapp.com/>.

- [35] Christian Szegedy, Wojciech Zaremba, Ilya Sutskever, Joan Bruna, Dumitru Erhan, Ian Goodfellow, and Rob Fergus. Intriguing properties of neural networks. *arXiv preprint arXiv:1312.6199*, 2013.
- [36] Hanlin Tang, Martin Schrimpf, William Lotter, Charlotte Moerman, Ana Paredes, Josue Ortega Caro, Walter Hardesty, David Cox, and Gabriel Kreiman. Recurrent computations for visual pattern completion. *Proceedings of the National Academy of Sciences*, 115(35):8835–8840, 2018.
- [37] Guillermo Valle-Perez, Chico Q. Camargo, and Ard A. Louis. Deep learning generalizes because the parameter-function map is biased towards simple functions. In *International Conference on Learning Representations*, 2019. URL <https://openreview.net/forum?id=rye4g3AqFm>.
- [38] Vladimir Vapnik. *The nature of statistical learning theory*. Springer science & business media, 1999.
- [39] Han Xiao, Kashif Rasul, and Roland Vollgraf. Fashion-MNIST: a novel image dataset for benchmarking machine learning algorithms. *arXiv preprint arXiv:1708.07747*, 2017.
- [40] Sangdoon Yun, Dongyoon Han, Seong Joon Oh, Sanghyuk Chun, Junsuk Choe, and Youngjoon Yoo. Cutmix: Regularization strategy to train strong classifiers with localizable features. In *Proceedings of the IEEE International Conference on Computer Vision*, pages 6023–6032, 2019.
- [41] Hongyi Zhang, Moustapha Cisse, Yann N. Dauphin, and David Lopez-Paz. mixup: Beyond empirical risk minimization. In *International Conference on Learning Representations*, 2018. URL <https://openreview.net/forum?id=r1Ddp1-Rb>.
- [42] Tianyuan Zhang and Zhanxing Zhu. Interpreting adversarially trained convolutional neural networks. In *International Conference on Machine Learning*, pages 7502–7511. PMLR, 2019.
- [43] Zhun Zhong, Liang Zheng, Guoliang Kang, Shaozi Li, and Yi Yang. Random erasing data augmentation. In *Proceedings of the AAAI Conference on Artificial Intelligence*, number 34(07), pages 13001–13008, 2020.

A Experimental details

Throughout the paper, we use PreAct-ResNet18 [16] models, trained for 200 epochs with a batch size of 128. For the MSDA parameters we use the same values as Harris et al. [15]. All models are augmented with random crop and horizontal flip and are averaged across 5 runs. We optimise using SGD with 0.9 momentum, learning rate of 0.1 up until epoch 100 and 0.001 for the rest of the training. This is due to an incompatibility with newer versions of the PyTorch library of the official implementation of Harris et al. [15], which we use as a starting point for model training. However, the difference in learning rate schedule between our work and prior art does not affect our findings since we are not introducing a new method to be applied at training time. In our case, it is sufficient to show that the bias exists in at least one configuration. For the analysis we also used adapted code from [3] for patch-shuffling. The models were trained on either one of the following: Titan X Pascal, GeForce GTX 1080ti or Tesla V100. For the analyses, a GeForce GTX 1050 was also used. The average training time was less than two hours, with the exception of model trained on Tiny-ImageNet, which took around 10 hours to run.

Training models

The code for model training is largely based on the open-source official implementation of FMix, which also includes those of MixUp, CutOut, and CutMix. For the experiment where we use the reformulated objective to combine data sets, instead of mixing with a permutation of the batch, as it is done in the original implementation of the mixed-augmentations, we now draw a batch from the desired data set. To ensure a fair comparison, for the basic we also perform inter-batch mixing.

Table 9: Alternative DI index for PreAct-ResNet18 on grid-shuffled images for four different types of models. Again, a bias can be noted for all considered data sets.

	basic	MixUp	FMix	CutMix
CIFAR-10	3.52 \pm 0.56	3.31 \pm 0.82	0.76 \pm 0.16	0.43 \pm 0.13
CIFAR-100	1.40 \pm 0.38	1.09 \pm 0.29	0.38 \pm 0.21	0.16 \pm 0.08
FashionMNIST	1.56 \pm 0.39	3.57 \pm 1.35	1.65 \pm 0.35	0.82 \pm 0.13
Tiny ImageNet	3.01 \pm 0.48	2.24 \pm 0.30	2.34 \pm 1.86	11.45 \pm 10.54
ImageNet	0.82	1.49	0.58	–

Table 10: Shape and texture accuracy of BagNet9 models on the GST data set.

	Shape	Texture
basic	11.29 \pm 0.15	18.90 \pm 0.66
MixUp	11.04 \pm 0.29	12.56 \pm 1.26
FMix	11.06 \pm 0.48	17.47 \pm 1.74
CutMix	10.76 \pm 0.27	20.28 \pm 0.88

Table 11: DI index for alternative grid sizes.

		basic	MixUp	FMix	CutMix
CIFAR-10	2 \times 2	0.61 \pm 0.24	0.56 \pm 0.33	0.19 \pm 0.14	0.12 \pm 0.06
	8 \times 8	6.41 \pm 0.55	6.95 \pm 1.96	2.75 \pm 1.46	1.41 \pm 1.15
CIFAR-100	2 \times 2	1.03 \pm 0.29	0.46 \pm 0.14	0.21 \pm 0.14	0.12 \pm 0.07
	8 \times 8	9.16 \pm 6.15	3.10 \pm 4.59	1.62 \pm 0.89	0.65 \pm 0.50
Tiny ImageNet	8 \times 8	5.76 \pm 6.61	5.73 \pm 3.82	2.49 \pm 1.38	0.60 \pm 0.69
	16 \times 16	44.01 \pm 36.47	14.06 \pm 14.63	11.94 \pm 17.79	1.86 \pm 1.98
ImageNet	16 \times 16	0.72	1.38	0.55	–
	64 \times 64	4.89	41.16	12.77	–

Evaluating robustness

For the CutOcclusion measurement, we modify open-source code to restrict the occluding patch to lie within the margins of the image to be occluded. This is to ensure that the mixing factor λ matches the true proportion of the occlusion. For iOcclusion, the implementation of Grad-CAM is again adapted from publicly available code. With both methods, we evaluate 5 instances of the same model and average over the results obtained.

The added computation time of iOcclusion over the regular CutOcclusion for a fixed occlusion fraction is that of performing Grad-CAM on train and test data, as well as evaluating on the latter. With a batch size of 128, this takes under half an hour.

B Analysis of wrong predictions

B.1 Alternative index

Table 9 the worst-case DI index where we replace $i_{c_{max}}$ in Equation 1 by the maximum increase across the runs. As per the original formulation, we note that the masking methods lead to models which are less sensitive to the artefacts resulted after patch-shuffling.

B.2 Varying the grid size

Table 11 gives the results obtained when varying the number of image tiles to be randomly rearranged. We observe that data interference appears for different grid sizes.

B.3 Patch-shuffling

We look at the classes which have the highest increase in incorrect predictions and note that their shapes are characterised by strong horizontal and vertical edges. For example, on CIFAR-100, varying the grid size between 2 \times 2, 4 \times 4 and 8 \times 8 gives "Lamp", "Bus" and "Table" as dominant c_{max} classes, while the model trained on Fashion MNIST with the standard procedure tends to predict grid-shuffled images as "Bag". Figure 5 shows that on ImageNet, the basic model tends to wrongly identify the patch-shuffled images as belonging to class "Envelope".

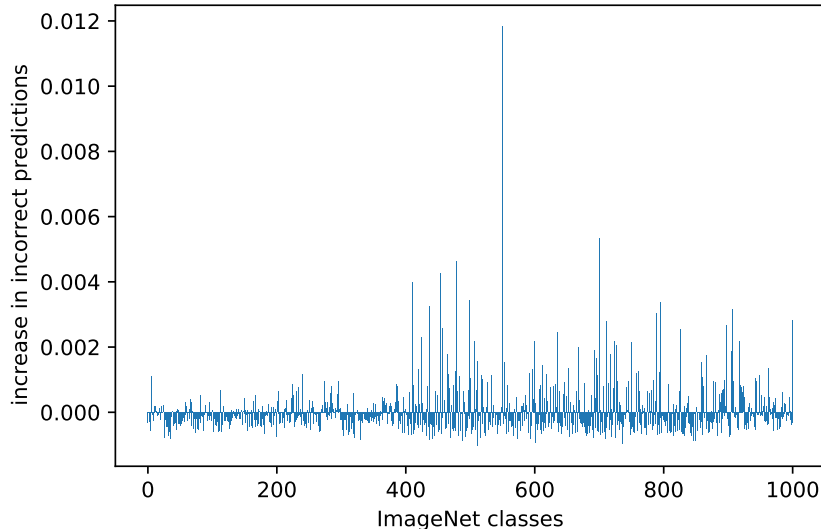


Figure 5: Difference between the number of times a class was wrongly predicted when presented with regular ImageNet samples and patch-shuffled data.

Table 12: DI index for occluding with images from another data set.

	basic	MixUp	FMix	CutMix
CIFAR-10	0.18 ± 0.05	0.39 ± 0.15	0.12 ± 0.11	0.08 ± 0.06
CIFAR-100	0.48 ± 0.09	0.61 ± 0.27	0.90 ± 0.15	1.25 ± 0.25
Fashion MNIST	3.40 ± 0.29	3.06 ± 1.07	1.81 ± 0.55	2.61 ± 0.80
Tiny ImageNet	0.25 ± 0.12	0.17 ± 0.04	0.06 ± 0.03	0.12 ± 0.04

B.4 CutOcclusion

In this section we experiment with alternative masking methods when computing CutOcclusion. We note that the bias exists when occluding with patches taken from images belonging to different data sets (Table 12). Figure 6 gives a visual account of the results obtained for CIFAR-10 when mix-patching. Note that for Fashion MNIST we use MNIST, for Tiny ImageNet we use ImageNet, while for CIFAR-10 we mix with CIFAR-100 and vice versa. Since ImageNet images are significantly larger than those of the other data sets, mixing would imply padding large areas, which would give results very similar to uniform patching. We also experiment with VGG models, where on CIFAR-10 the basic has a DI index of 0.80 ± 0.40 compared to 0.18 ± 0.11 of MixUp. We then use masks sampled from Fourier space (Table 13) and note that even for these irregularly shaped distortions, we can identify a gap in most cases. The only exception is in the case of Fashion MNIST. It must be stressed that although all the models we experimented with presented Data Interference for this problem, this does not exclude the possibility of constructing a different model that is insensitive to this distortion. For example, we identify a gap for this problem when mix-masking (DI index of 4.09 ± 1.74 for the basic model as opposed to 1.87 ± 0.27 for a model trained on images that were masked out using FMix-like masks). Thus, when occluding with a particular shape we implicitly disfavour models in which learnt representations are related to the features introduced by that shape.

Figure 8 also gives the results for CutOcclusion and iOcclusion for training with 3 random masks sampled from Fourier space.

B.4.1 BagNet shape and texture accuracy

We evaluate on the GST data set BagNet9 models trained on Tiny ImageNet and present the results in Table 10. Despite the basic model displaying a bias towards predicting one of the classes when presented with patch-shuffled images (see Figure 9), once again it does not have a lower texture or higher shape bias than the masked-based augmentations.

Table 13: DI index for patching using masks sampled from Fourier space.

	basic	MixUp	FMix	CutMix
CIFAR-10	2.08 ± 1.13	1.79 ± 1.09	1.32 ± 0.99	4.21 ± 1.23
CIFAR-100	4.06 ± 0.47	3.11 ± 0.29	9.90 ± 14.32	2.89 ± 0.36
Fashion MNIST	49.55 ± 20.45	40.69 ± 21.63	27.87 ± 17.57	61.04 ± 17.92
Tiny ImageNet	4.37 ± 0.85	6.95 ± 1.84	3.60 ± 1.73	5.92 ± 4.38
ImageNet	3.27	2.24	6.08	—

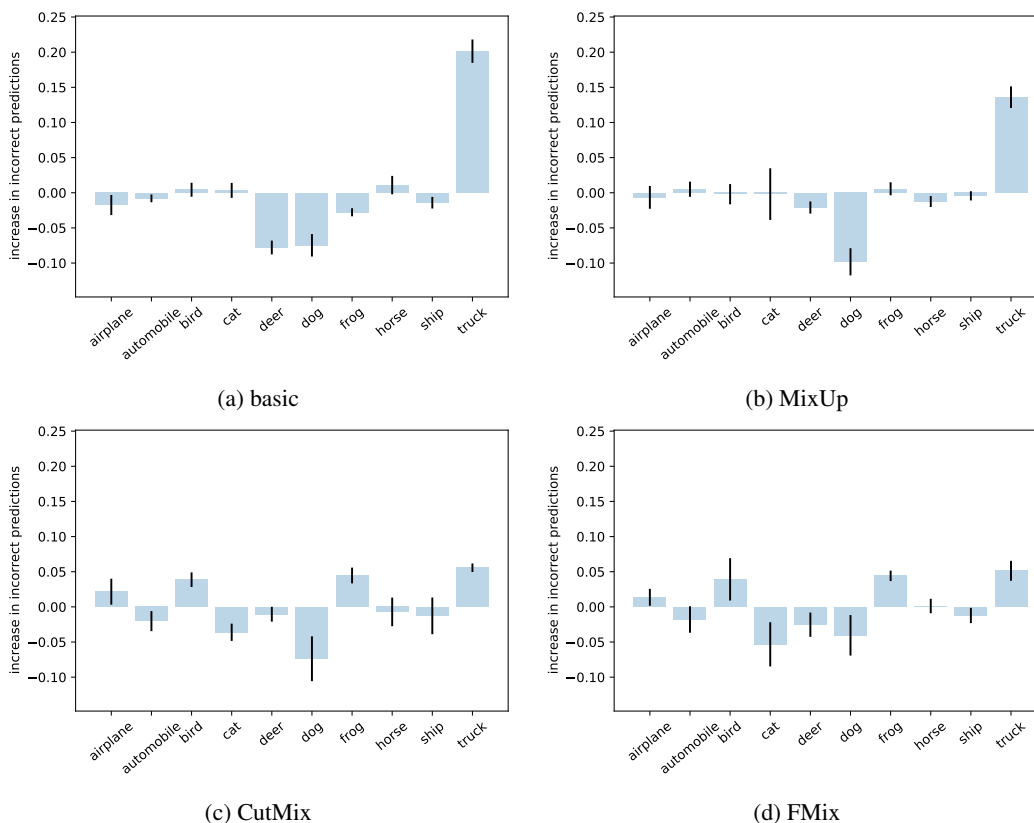


Figure 6: Difference between wrongly predicted classes when testing on original data versus CutMix images. The evaluated models from left to right, top to bottom are trained on CIFAR-10 with: no mixed-data augmentation (basic), MixUp, CutMix, and FMix.

C Further results on iOcclusion experiments

C.1 Alternative CutOcclusion

Table 14 gives the DI index when forcing the occluding patch to lie within image boundaries for patch sizes sampled from Beta(2,1). For the same scenario, but sampling uniformly from [0.1, 1] we present results in Table 15. Note that in the case of Tiny ImageNet the bias is more visibly present for larger occluders. As such, uniformly sampling the patch size from the interval [0.3, 1] results in a DI index of 13.46 ± 5.74 for the basic model, while the level of data interference from MixUp is only 4.75 ± 1.93 . Similarly, for Fashion MNIST, when we increase the size of the occluder we obtain 0.65 ± 0.20 for Mixup as opposed to 0.07 ± 0.11 for the basic model. However, this does not change the conclusions of our experiments since, as mentioned in the main paper, robustness studies are usually carried out with large occluder sizes.

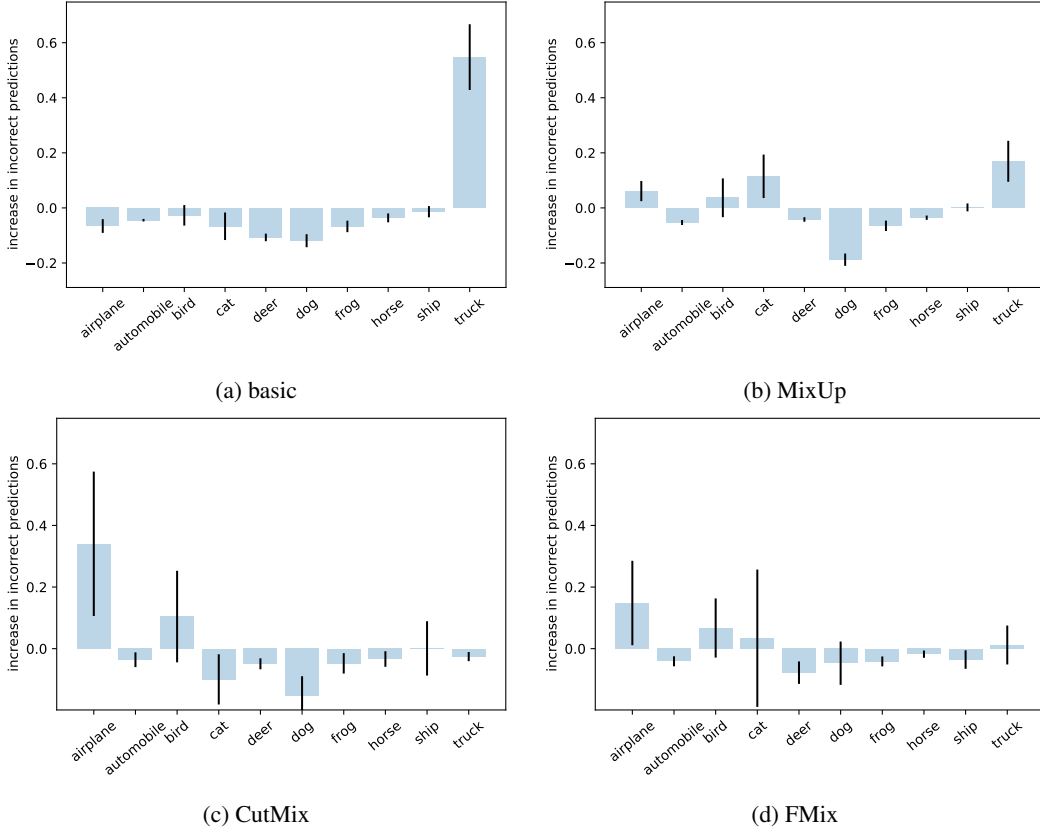


Figure 7: Difference between wrongly predicted classes when testing on original data versus CutOut images. The evaluated models from left to right, top to bottom are trained on CIFAR-10 with: no mixed-data augmentation (basic), MixUp, CutMix, and FMix.

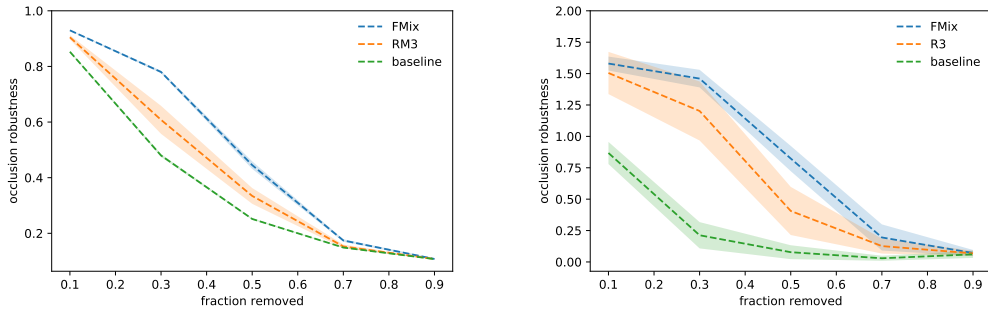


Figure 8: CutOcclusion (left) and iOcclusion (right). Note that there is a difference in scale and the two should not be directly compared. We are rather interested in how the methods situate the different augmentation with respect to each other. It is important to notice that when measuring the robustness with CutOcclusion, RM3 appears significantly less robust than FMix due to its sensitivity to patching with rectangles. On the other hand, iOcclusion highlights the robustness specific to FMix.

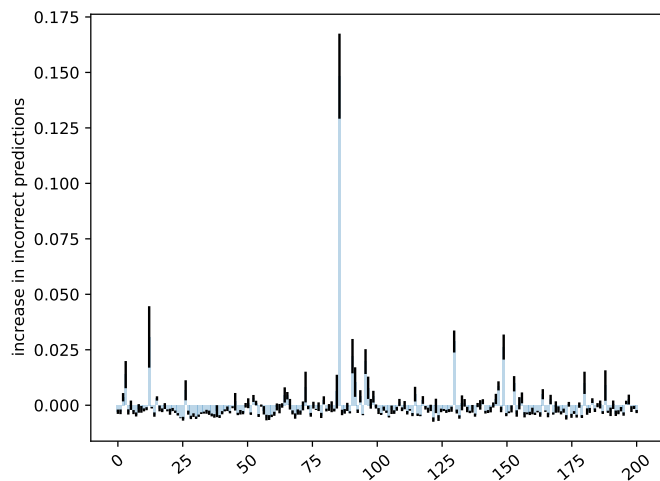


Figure 9: Difference between wrongly predicted classes when testing on original Tiny ImageNet data versus CutOut images.

Table 14: DI index for sampling occluder size from a uniform distribution when the patch is restricted to lying within image boundaries and the size is sampled from Beta(2,1).

	basic	MixUp	FMix	CutMix
CIFAR-10	5.88 ± 1.82	0.76 ± 0.69	1.30 ± 1.27	3.68 ± 3.66
CIFAR-100	29.71 ± 10.19	6.80 ± 7.55	6.08 ± 6.28	13.19 ± 25.85
Fashion MNIST	0.67 ± 0.38	3.51 ± 1.38	1.87 ± 3.33	1.78 ± 2.93
Tiny ImageNet	15.25 ± 4.84	6.38 ± 4.03	5.87 ± 6.07	13.97 ± 24.02
ImageNet	9.93	28.72	11.52	—

Table 15: DI index for sampling occluder size from a uniform distribution when the patch is restricted to lying within image boundaries and the size is sampled from [0.1, 1] uniformly.

	basic	MixUp	FMix	CutMix
CIFAR-10	5.74 ± 1.86	0.75 ± 0.69	1.25 ± 1.24	3.61 ± 3.60
CIFAR-100	28.63 ± 9.85	6.31 ± 7.03	5.86 ± 5.86	12.63 ± 24.69
Fashion MNIST	1.88 ± 3.36	3.54 ± 1.33	1.91 ± 3.33	1.76 ± 2.91
Tiny ImageNet	1.406 ± 04.36	0.581 ± 03.32	0.553 ± 05.66	1.249 ± 21.44
ImageNet	0.25	0.48	0.14	—

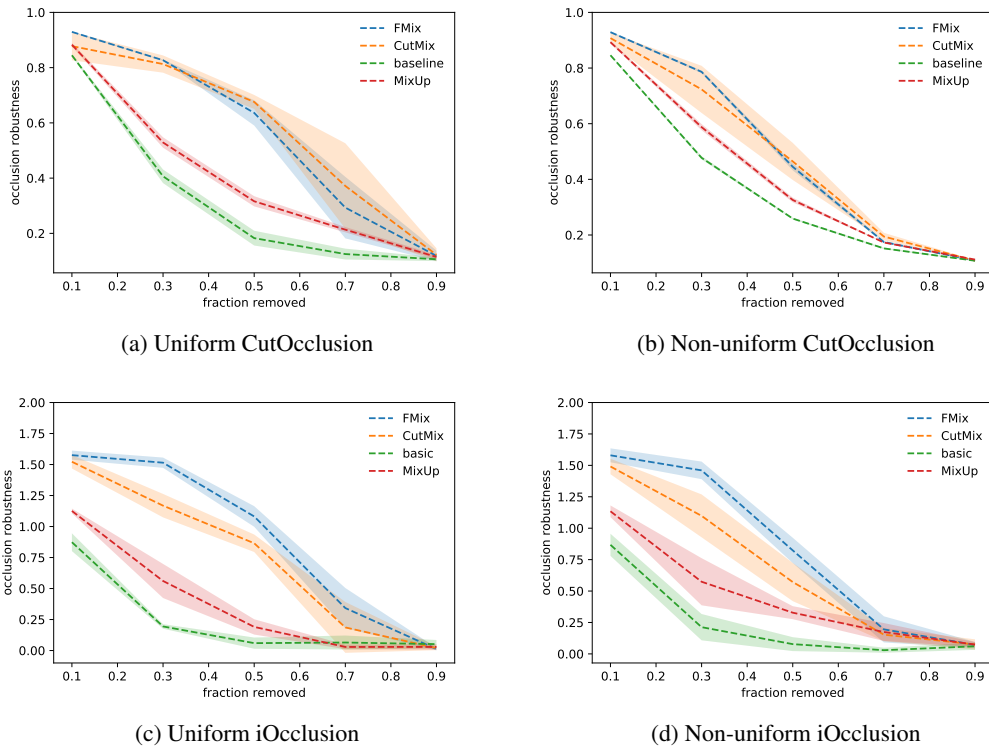


Figure 10: Comparison of metric sensitivity to textured occlusion. Uniform occlusion refers to superimposing uniform patches over CIFAR-10 images, while nonuniform refers to superimposing part of CIFAR-100 samples. Nonuniform CutOcclusion provides significantly different results to its regular counterpart.

C.2 Occluding with images from another data set

Since CutOcclusion does not account for the bias introduced by the occluding method, it is expected that changing the patch to a non-uniform one would greatly affect the results. For CIFAR-10 models, Figure 10 presents the results of occluding with CIFAR-100 images. iOcclusion better rules out the specifics of the occluding patch, its uniform version giving similar results to the non-uniform one, whereas CutOcclusion pushes everything together.

C.3 Randomising labels

To assess the sensitivity of CutOcclusion and iOcclusion to the overall performance of the model, we also experiment with randomising all the labels of the CIFAR-10 data set. When evaluated on the unaugmented training data, all the basic models achieve 100% accuracy, while the FMix models reach 99.99 ± 0.01 . Since all labels are corrupted, the accuracy on the test set before and after occlusion is no greater than random. However, the robustness of the augmentation-trained model can be seen on the training data, as captured by our metric (See Figure 11). On the other hand, CutOcclusion makes no distinction between learning with regular and augmented data (Table 16). Despite being such a peculiar case, it shows the comprehensiveness gained by accounting for the degradation on test data in relation to that on train.

C.4 Approximating iOcclusion

As alternative methods for computing iOcclusion we experiment both with masks sampled from Fourier space and randomly positioned square patches. Although using this type of random masking methods for computing \mathcal{D}_{train}^i and \mathcal{D}_{test}^i in Equation (1) gives less precise results, it has the advantage of incurring less computation and can be used for rapid model analysis. For assessing a model across

Table 16: Robustness to occluding with patches covering 50% of each image. The models are trained with and without masking augmentation on data with randomised labels. CutOcclusion makes no difference between regular and augmented training.

	basic random	FMix random	FMix clean
CutOcclusion	10.24 \pm 0.27	9.78 \pm 0.18	63.63 \pm 4.54
iOcclusion	14.63 \pm 1.12	47.94 \pm 19.84	82.36 \pm 10.06

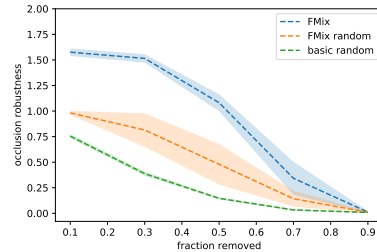
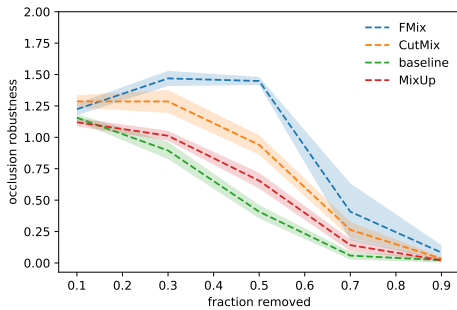
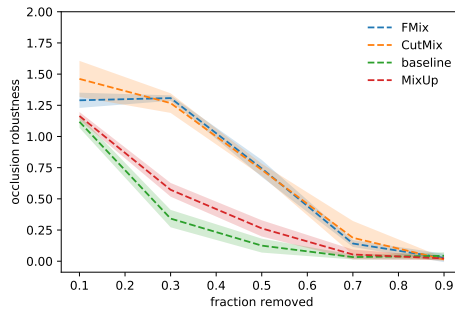


Figure 11: iOcclusion results for training with clean and corrupted labels for basic and FMix augmentation.



(a) Fourier-sampled patches



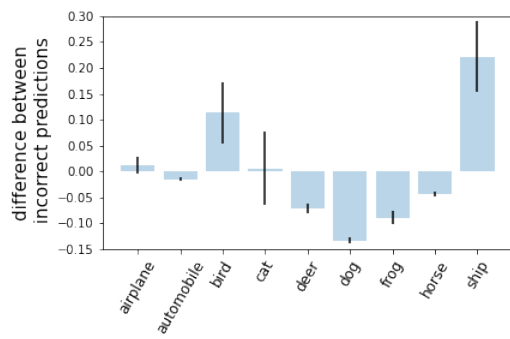
(b) Rectangular patches

Figure 12: Approximating iOcclusion with random masking can provide a first intuition, but is significantly noisier than using a saliency method.

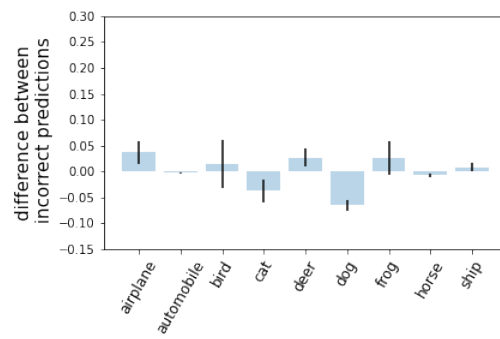
5 runs for 6 different levels of occlusion, this method leads to a carbon footprint of 0.05 kgCO₂eq as opposed to 1.04 using Grad-CAM. In Figure 12 we present the results obtained with these alternatives. We expect both methods to provide overoptimistic results for small patches, while Fourier sampling is expected to give more truthful scores as the size of the patch increases. On the other hand, the contiguity of CutOut-based occlusion comes at the cost of not determining the robustness to multiple simultaneous occluders. This seems to play a role especially in the case of CutMix augmentation. Indeed, when superimposing a rectangular patch, it is difficult to differentiate CutMix from FMix-trained models. To confirm that this is caused by the granularity of the occluders and not the shape, we also experiment with occluding using multiple rectangular patches. We split the images in a 4 × 4 grid and occlude i% of the tiles, obtaining results that are more similar to those obtained when occluding with Fourier-sample patches. Thus, while significantly noisier, using randomly positioned occluders can provide an alternative for computing iOcclusion given that one takes into account the number of occluders.

D Removing the dominant class

We remove the 10th class from the CIFAR-10 data set and retrain on the remaining classes. In the main paper we give the results for occluding with non-uniform patches. When using black patches to obstruct images, we again identify a gap, but this time with respect to a CutOut-trained model (see Figure 13). The basic model has a DI index of 1.23 \pm 0.72, while CutOut 0.13 \pm 0.10. Thus, in both cases a model that is less affected by the artefacts than the basic model can be found. Thus, when measuring CutOcclusion, the basic model will be disadvantaged.



(a) Fourier-sampled patches



(b) Rectangular patches

Figure 13: Difference in incorrect predictions for the basic (left) and CutOut(right) models.